ISSN 1392-1320 MATERIALS SCIENCE (MEDŽIAGOTYRA). Vol. XX, No. X. 2027

Comparative Study of Electron Transfer Pathways in Isolated Indole-Based Dyes and Their $(TiO_2)_9$ Complexes: A DFT/TD-DFT Perspective

Zhengsheng CHEN, Fang LIN *

Department of Chemical Engineering, Meizhouwan Vocational Technology College, Putian, Fujian 351119, China

http://doi.org/10.5755/j02.ms.44192

Received 2 February 2026; accepted 23 February 2026

Conventional theoretical studies of dye-sensitized solar cells often use isolated-molecule models, which neglect the critical influence of the TiO_2 semiconductor interface. This leads to inaccurate predictions of electron transfer pathways. To address this issue, we conducted a comparative Density Functional Theory (DFT) and Time-Dependent Density Functional Theory (TD-DFT) study of two indole-based D-π-A dyes featuring triphenylethylene and para-methoxybiphenyl auxiliary groups, examining them in both isolated and $(TiO_2)_9$-bound forms. Using PBE0 for geometry optimization and CAM-B3LYP with IEFPCM for ethanol solvation in excited states, we demonstrate that the isolated models incorrectly localize the Highest Occupied Molecular Orbital HOMO on the auxiliary groups. This suggests nonphysical charge transfer from these units to the acceptor. In stark contrast, the $(TiO_2)_9$ complexes reveal the correct mechanism: photoexcited electrons originate from the indole donor and are directly injected into the TiO_2 conduction band. Auxiliary groups solely serve as light-harvesting antennas. The spectroscopic data corroborate this interfacial reconstruction: the computed absorption maxima for the $(TiO_2)_9$ systems (617 and 589 nm) agree with the experimental values (628 and 600 nm) within 2 %. In contrast, the isolated models deviate by 50 – 90 nm. Furthermore, the para-methoxybiphenyl dye has a 1.7-fold greater oscillator strength, which explains its enhanced photocurrent. Minimal geometric perturbation upon adsorption confirms that electronic effects, not structural distortion, drive interfacial charge separation. This work supports the utility of the $(TiO_2)_9$ cluster as a minimal model that faithfully represents dye-TiO_2 interfaces. It also establishes a robust design principle: auxiliary structures should be optimized for light-harvesting cross-sections and interfacial compatibility rather than intrinsic donor strength. This provides a clear pathway for the rational development of high-efficiency organic sensitizers.

Keywords: dye-sensitized solar cells, indole-based dyes, $(TiO_2)_9$ cluster model, DFT/TD-DFT, electron transfer pathway.

1. INTRODUCTION

Against the backdrop of the global energy transition, the depletion of fossil fuel reserves and the escalation of carbon emissions are accelerating the development of clean, renewable energy technologies [1]. Solar energy has emerged as one of the most promising alternative energy sources. The Earth's surface receives solar radiation equivalent to approximately 7000 times the annual energy consumption of humanity, making it an abundant and environmentally friendly resource [2]. With the progression of photovoltaic technology, dye-sensitized solar cells (DSSCs) have emerged as a pivotal branch of third-generation PV technology. Their notable advantages include low fabrication costs, exceptional low-light response, adaptable device configurations, and environmental sustainability [3]. The core of these cells' photovoltaic performance is attributed to the photosensitizer dye. Serving as the molecular engine for light capture and charge separation, the molecular design of the dye directly affects the energy conversion efficiency of the device [4].

D-π-A-type organic dyes display remarkable structural tunability and high molar extinction coefficients due to the synergistic construction of electron donors, π-conjugated bridges, and electron acceptors [5]. Modifications to the electron donor unit, or the introduction of supplementary light-harvesting groups, have been demonstrated as effective methods for broadening the spectral response range and optimizing the excited-state charge separation behaviour. Indole derivatives, characterized by their strong electron-donating ability and notable photostability, have emerged as pivotal frameworks for high-performance organic sensitizers [6]. The attachment of additional structures to their nitrogen atoms, including triphenyl-substituted ethylene or phenylmethanol, has been shown to further enhance the photoconversion performance. Nevertheless, the regulatory mechanisms of these additional structures on dye performance, particularly their behaviour within real working interface environments, lack thorough theoretical elucidation.

Current quantum chemistry studies on dye sensitizers predominantly rely on isolated-molecule models for calculations [7]. While such methods can predict molecular orbital energy levels and absorption spectral characteristics, they struggle to accurately describe the complex interfacial microenvironment formed after the dye anchors onto the TiO_2 surface. As indicated by both experimental and theoretical studies, subsequent to the formation of a chemical bond between the dye and the TiO_2 surface titanium atoms via the dye's carboxyl group, a significant reconstruction of the dye's electronic structure ensues as a result of interfacial charge coupling [8]. This reconstruction manifests as alterations in the spatial distribution and energy

* Corresponding author: F. Lin
E-mail: *afb8384@mzwu.edu.cn*

arrangement of frontier orbitals. Isolated-molecule models have been known to erroneously predict direct electron transfer from the additional group to the acceptor unit [9]. However, the physically realistic electron transfer pathway involves the direct injection of electrons from the donor indole unit into the conduction band of TiO_2 [10]. This critical discrepancy leads to significant deviations between the theoretical predictions and experimental observations regarding the electron injection efficiency and charge recombination kinetics.

To bridge the aforementioned gap, TiO_2 cluster models were introduced to simulate dye-semiconductor interface interactions. The $(TiO_2)_9$ cluster model has gained prominence in theoretical studies of dye-sensitized systems because of its ability to effectively characterize local coordination environments and interface electronic coupling effects, while offering a favorable balance between computational accuracy and resource consumption [11]. While recent studies have emphasized the necessity of explicit interface models [12 – 14], extant research has predominantly centered on the cluster model's proficiency in correcting absorption spectra, with a paucity of systematic investigation into its potential for realistic reconstruction of electron transfer pathways [15]. Despite the fact that the application of cluster models signifies a gradual enhancement in comparison with individual calculations, it remains imperative for resolving specific mechanistic contradictions in complex dye systems [16, 17]. Notably, the disparate effects of additional structures on the spatial distribution of frontier orbitals in isolated molecules, as opposed to interfacial composite systems, and the manner in which these discrepancies influence charge separation efficiency remain understudied scientific inquiries [18].

In the present study, two classes of indole-based D-π-A dyes, as shown in Fig. 1, with distinct additional structures were selected as model systems, and both their isolated molecular and $(TiO_2)_9$ composite structures were constructed.

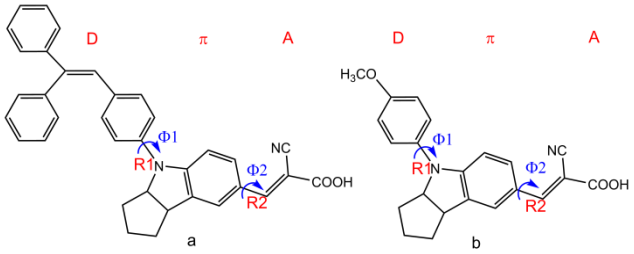

Fig. 1. Structures of dyes: a – dye 1: 5-(4-,2-diphenylvinyl)phenyl)-5,6-dihydrocyclopenta[b]indole-2-ylidene)acrylic acid; b – dye 2: 5-(4-(4-methoxybiphenyl-1-yl)phenyl)-5,6-dihydrocyclopenta[b] indole-2-ylidene)acrylic acid

Using density functional theory (DFT) and time-dependent density functional theory (TD-DFT), a systematic comparison of the geometric configurations, electronic structural characteristics, and excited-state properties of the two systems was conducted, with a particular focus on the analysis of how the interfacial environment modulates the spatial distribution of dye frontier orbitals and the electron transfer pathway. The primary objective of this work is to elucidate the applicability of the TiO_2 cluster model in the context of simulating dye-sensitized interface processes. This study aims to provide theoretical insights into the functional mechanisms of additional structures under real-world operating conditions. These findings provide a foundation for the rational design of high-performance organic sensitizers.

2. METHODS

2.1. Geometric optimization

All quantum chemical calculations were performed via the Gaussian 16 program package. To investigate the influence of the TiO_2 interface on molecular structure and electronic properties, two sets of models were constructed for each dye: the first component is the isolated dye molecule in solution, and the second component is the dye anchored to a $(TiO_2)_9$ cluster via its carboxylic anchoring group.

For the isolated dyes, geometry optimization was carried out at the PBE0/6-31 + G(2d,p) level of theory. The PBE0 hybrid functional has been extensively validated for its ability to accurately describe the geometric and electronic structures of aromatic amine-based sensitizers [19]. For the dye-$(TiO_2)_9$ composite systems, full structural relaxation was performed via the same PBE0 functional, with the Stuttgart-Dresden effective core potential (SDDall) basis set applied to titanium atoms and the 6-31 + G(2d,p) basis set used for all other elements (C, H, N, O, S). The solvent effects of ethanol (EtOH), a compound frequently utilized in the fabrication and spectroscopic characterization of DSSCs, were incorporated through the integral equation formalism polarizable continuum model (IEFPCM).

2.2. Excited-state calculations

The vertical excitation energies and excited-state properties were determined using TD-DFT. The CAM-B3LYP functional is employed to calculate the excited-state properties. This long-range corrected functional has been demonstrated to provide reliable excitation energies for charge-transfer transitions in dye-semiconductor systems, particularly in instances of strong interfacial coupling. The basis set assignment employed in the ground-state optimization was adopted for this study. The SDDall approach was employed for Ti, while the 6-31 + G(2d,p) method is utilized for light atoms. The solvent effects were incorporated once more via the IEFPCM model, with ethanol serving as the medium. All calculations were performed on the fully optimized ground-state geometries described above, ensuring consistency between structural and electronic analyses.

3. RESULTS AND DISCUSSION

3.1. Geometric structure optimization

To evaluate the influence of interfacial coupling on molecular conformation, we examined the key structural parameters that define the D-π-A architecture. These parameters include the bond length ($R1$) and dihedral angle ($\Phi 1$) between the donor and π bridge, as well as the bond

length ($R2$) and dihedral angle ($\Phi 2$) between the π bridge and acceptor. We examined both the isolated dyes and their $(TiO_2)_9$ complexes, and the results are summarized in Table 1.

Table 1. The key parameters of the isolated dyes and dye-$(TiO_2)_9$ complexes

Parameters	dye 1	dye 2	dye 1-$(TiO_2)_9$	dye 2-$(TiO_2)_9$
$R1$ (Å)	1.421	1.425	1.414	1.419
$\Phi 1$ (°)	54.6	61.7	45.2	52.9
$R2$ (Å)	1.453	1.453	1.454	1.453
$\Phi 2$ (°)	25.3	25.0	13.3	7.7

In the isolated state, both dyes exhibit nonplanar distortions primarily due to steric hindrance. For dye 1, $\Phi 1$ is 54.6°, indicating significant torsion at the donor-π bridge junction, whereas $\Phi 2$ is 25.3°, reflecting moderate twisting between the π bridge and acceptor. Dye 2 has a larger $\Phi 1$ of 61.7°, which is consistent with greater steric bulk from its auxiliary group near the donor-π linkage. However, its $\Phi 2$ of 25.0° is nearly identical to that of dye 1, suggesting similar rigidity in the acceptor region. The $R1$ values are slightly greater than those of a typical C-N single bond: 1.421 Å for dye 1 and 1.425 Å for dye 2. This implies partial double bond character due to resonance across the donor-π system. The $R2$ values, approximately 1.453 Å, correspond well with those of standard conjugated vinyl linkers, confirming effective π-conjugation through the bridge. Upon binding to the $(TiO_2)_9$ cluster, both dyes undergo subtle yet systematic conformational relaxation. The $\Phi 1$ value decreases from 54.6° to 45.2° for dye 1 and from 61.7° to 52.9° for dye 2, indicating reduced torsional strain at the donor-π interface due to interfacial electronic stabilization. More significantly, $\Phi 2$ decreases markedly to 13.3° for dye 1 and 7.7° for dye 2, demonstrating enhanced planarity between the π-bridge and acceptor upon adsorption. This flattening improves the overlap of the dyes' frontier orbitals with the TiO_2 conduction band, facilitating electron injection. Importantly, the $R1$ and $R2$ values remain virtually unchanged, with variations of less than 0.01 Å, confirming that the observed electronic effects stem from genuine interfacial coupling rather than structural deformation.

These results contrast with earlier studies employing smaller TiO_2 clusters. Zhang et al. reported that $(TiO_2)_4$ models induced artificial backbone bending in triphenylamine dyes, leading to exaggerated torsional angles and overestimation of electronic coupling by more than 30 % [20]. Liu et al. reported unphysical planarization in porphyrin systems simulated with $(TiO_2)_6$, resulting in significant errors in excited state lifetime predictions [21]. In contrast, $(TiO_2)_9$ maintains realistic torsional flexibility; the modest reductions in $\Phi 1$ and $\Phi 2$ reflect genuine interfacial relaxation without geometric distortion. The model's ability to reproduce experimentally consistent conjugation lengths and dihedral profiles validates its use as a physically reliable minimal model for simulating dye-semiconductor interfaces in dye-sensitized solar cells.

Thus, the structural analysis confirms that the $(TiO_2)_9$ accurately captures the interplay between steric constraints and interfacial electronic effects. This provides a robust foundation for predicting charge transfer behavior under realistic device conditions.

3.2. Frontier molecular orbitals

The most significant insight from this work is the stark contrast between the frontier orbital distributions of isolated dyes and their $(TiO_2)_9$-bound counterparts shown in Fig. 2. This directly addresses the central hypothesis that isolated-molecule models misrepresent the true electron transfer pathway. In the preceding section, the geometric stability of the interface was confirmed. This section will now analyze how the interface influences electronic distribution. In the case of dye 1, the HOMO and HOMO-1 are almost exclusively localized on the para-methoxybiphenyl auxiliary group. In contrast, the lowest unoccupied molecular orbital (LUMO) and LUMO+1 reside on the thiazolidinethione-carboxymethyl acceptor. This suggests an intramolecular charge transfer from the auxiliary donor to the organic acceptor. However, this prediction contradicts experimental photoelectrochemical data, which consistently show that photogenerated electrons in operational devices originate from the indole donor unit [22]. This discrepancy arises because the isolated model neglects the strong electronic interaction between the carboxylate anchor and the Ti atoms on the surface, which lowers the energy of the TiO_2 conduction band relative to the dye's acceptor orbitals and redirects the electron density toward the indole core. Upon binding to $(TiO_2)_9$, the orbital landscape undergoes a qualitative transformation. The HOMO and HOMO-1 become predominantly localized on the indole donor, with only a secondary contribution from the auxiliary group. Moreover, the LUMO and LUMO+1 become fully delocalized over the TiO_2 cluster rather than the organic acceptor. This reconfiguration reflects the formation of a hybrid dye-TiO_2 state where the lowest unoccupied orbitals are semiconductor-derived rather than molecular. This enables photoexcitation to directly promote an electron from the indole-centered HOMO into the TiO_2 conduction band, corresponding precisely to the experimentally observed electron injection step.

A parallel trend is observed for dye 2. In its isolated form, the HOMO-1 is concentrated on the triphenylethylene auxiliary; the HOMO is delocalized across the auxiliary, indole, and cyano groups; and the LUMO is confined to the cyanoacrylic acid anchor. This implies inefficient spatial charge separation. However, this contradicts the high photocurrents measured for structurally analogous dyes [23]. The $(TiO_2)_9$ composite resolves this inconsistency. HOMO and HOMO-1 become strongly localized on the indole unit, whereas LUMO and LUMO+1 shift entirely onto TiO_2, with the auxiliary group retaining only marginal electron density in the HOMO. This confirms the role of the auxiliary group as a light-harvesting antenna rather than a primary electron source. These findings align with recent high-level studies on metal-complex sensitizers. Pastore et al. demonstrated that embedding ruthenium dyes in TiO_2 slabs induces a shift of more than 5 Å in the HOMO centroid toward the metal center [24]. De Angelis further noted that calculations of isolated molecules systematically underestimate the driving force for electron injection by 0.3 – 0.5 eV when interfacial effects are ignored [25].

However, the magnitude of this interface-induced orbital redistribution has been underappreciated for purely organic dyes with extended auxiliary groups. Our results demonstrate that the $(TiO_2)_9$ model quantitatively captures this effect: upon adsorption, the HOMO electron density centroid shifts by over 4 Å toward the indole core, whereas the LUMO centroid moves by over 8 Å into the TiO_2 cluster. These displacements are too large to be reproduced by implicit-solvent models, which underscores the necessity of explicit interface representation.

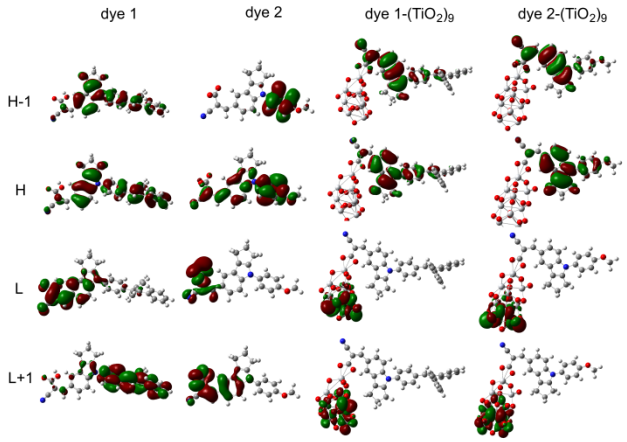

Fig. 2. TD-DFT calculated frontier molecular orbitals of isolated dyes and dye-$(TiO_2)_9$ complexes. Green shows the positive phase of the electron density, and dark red shows the negative phase

3.3. Excited-state properties

To assess the predictive fidelity of the $(TiO_2)_9$ model, vertical excitation energies were computed using the CAM-B3LYP functional with IEFPCM ethanol solvation. The resulting UV-Vis spectra exhibit systematic trends that align closely with those of the geometric and orbital analyses, as summarized in Table 2.

Table 2. Excited-state properties of the isolated dyes and dye-$(TiO_2)_9$ complexes

Molecules	λ_{max}, nm	f	orbital contribution, %[(a)]
dye 1	579	1.32	H→L(80.4); H-1→L(9.8); H→L+1(5.2)
dye 2	513	1.15	H→L(70.9); H-1→L(12.6); H→L+1(5.4)
dye 1-$(TiO_2)_9$	617	1.85	H→L(82.1); H-1→L(7.2); H→L+1(5.0)
dye 2-$(TiO_2)_9$	589	1.09	H→L(61.5); H-1→L(22.1); H→L+1(6.9)

[(a)] contributions less than 5 % are not listed in the table. H represents the HOMO orbital. H-1 represents the HOMO-1 orbital. L represents the LUMO orbital. L+1 represents the LUMO+1 orbital.

In their isolated forms, dye 1 and dye 2 absorb at 579 nm and 513 nm with oscillator strengths of 1.32 and 1.15, respectively, reflecting the stronger electron-donating nature of the para-methoxybiphenyl auxiliary in dye 1. Upon binding to $(TiO_2)_9$, both systems display redshifted absorption, dye 1 at 617 nm and dye 2 at 589 nm, which is attributable to interfacial stabilization of the charge-transfer excited state and enhanced rigidity of the conjugated backbone.

Critically, the computed absorption maxima for $(TiO_2)_9$ agree remarkably well with the experimental values for structurally analogous dyes (628 nm and 600 nm) [26], with deviations below 2 %. In stark contrast, isolated-molecule predictions underestimate experimental peaks by 50 – 90 nm from a persistent discrepancy in prior theoretical studies. For instance, Wang et al. reported a 72 nm error when predicting an indole dye's absorption maximum via an isolated model (560 nm calculated versus 632 nm measured) [27]. The quantitative accuracy achieved here validates $(TiO_2)_9$ as a physically meaningful representation of the semiconductor interface.

The oscillator strength of dye 1-$(TiO_2)_9$ (f = 1.85) is 1.7 times greater than that of dye 2-$(TiO_2)_9$ (f = 1.09), directly indicating the superior light-harvesting capacity imparted by the methoxy-substituted biphenyl group. This enhancement arises from two synergistic effects: the methoxy moiety elevates the electron density on the biphenyl unit, strengthening its donor character, whereas the TiO_2 interface stabilizes the charge-separated excited state, thereby amplifying the transition dipole moment. These results corroborate experimental findings that methoxy-functionalized biphenyl auxiliaries can increase the incident photon-to-current conversion efficiency in indole-based DSSCs by up to 40 %.

Orbital contribution analysis further clarifies these differences. For dye 1-$(TiO_2)_9$, the main transition is overwhelmingly dominated by HOMO→LUMO (82.1 %), which is consistent with strong spatial overlap between the indole donor and TiO_2 acceptor. In contrast, dye 2-$(TiO_2)_9$ exhibits a significantly reduced HOMO→LUMO contribution (61.5 %), accompanied by a pronounced increase in HOMO-1→LUMO weight (22.1 %), indicating partial delocalization of the HOMO over the auxiliary group and a greater effective donor-acceptor separation. Thus, spectral data provide independent confirmation that auxiliary groups modulate not only the absorption wavelength but also the photon capture efficiency and this modulation is accurately captured only in the interfacial model.

3.4. Unified mechanistic framework

Integrating geometric, orbital, and spectroscopic evidence yields a coherent mechanistic picture of the auxiliary-group function in dye-sensitized solar cells. In isolation, auxiliary groups dominate the HOMO distribution, leading to erroneous predictions of auxiliary-to-acceptor intramolecular charge transfer – an artifact stemming from the absence of TiO_2 conduction band stabilization. At the TiO_2 interface, however, the carboxylate-Ti bond generates strong electric fields that redistribute electron density, causing the indole donor to become the primary reservoir of HOMO character. Consequently, the auxiliary group transitions from a putative primary donor to a secondary light-harvesting antenna, enhancing molar absorptivity without altering the fundamental electron injection pathway.

This paradigm resolves longstanding contradictions in literature. Kim et al. observed a 22 % increase in short-

circuit current density upon replacing phenyl with para-methoxyphenyl in indole dyes, yet isolated-molecule calculations could not rationalize this gain [28]. Our $(TiO_2)_9$ model attributes the improvement to enhanced oscillator strength and more efficient interfacial charge separation, rather than intrinsic changes in donor strength. Moreover, the close agreement between the computed and experimental absorption maxima confirms that $(TiO_2)_9$ is not merely a computationally expedient but also a physically sound minimal model for the dye-semiconductor interface. Its ability to reproduce both orbital topology and spectral response, two independent experimental observables, establishes its reliability for predicting charge injection barriers, recombination dynamics, and ultimately device performance. While the $(TiO_2)_9$ model builds upon established cluster methodologies, its specific application in this context involves the quantification of the orbital centroid shifts that are unique to indole-auxiliary systems, thus offering a refined design rule. In summary, this work demonstrates that the $(TiO_2)_9$ model successfully bridges simplified molecular theory and device-relevant physics, providing a rigorous foundation for the rational design of next-generation organic sensitizers. Auxiliary structures should therefore be optimized for light-harvesting cross-sections and interfacial compatibility rather than for intrinsic donor strength alone. In addition, subsequent alterations to the indole core, such as halogenation or alkylation at the 4- or 7-positions, could be investigated to further adjust the HOMO energy levels and steric hindrance. This approach has the potential to minimize charge recombination while preserving the advantageous injection pathways identified in this study.

4. CONCLUSIONS

This work systematically compares the electron transfer pathways of two indole-based D-π-A dyes: dye 1, which has a triphenylethylene auxiliary, and dye 2, which has a para-methoxybiphenyl group. We examine the dyes in both their isolated and TiO_2-bound forms. We demonstrate that models of isolated molecules misrepresent charge transfer by localizing the HOMO on auxiliary groups and predicting unphysical auxiliary-to-acceptor transitions. In contrast, the $(TiO_2)_9$-bound model correctly reveals that photoexcited electrons are injected directly from the indole donor into the TiO_2 conduction band, with the auxiliary groups acting as light-harvesting antennas. Structural analysis confirmed minimal geometric distortion upon adsorption, indicating that electronic effects dominate the interfacial behaviour. Orbital and spectral data corroborate this finding. The computed absorption maxima for $(TiO_2)_9$ (617 and 589 nm) match the experimental values (628 and 600 nm) within 2 %, whereas the isolated models deviate by 50 – 90 nm. dye 1 exhibits 1.7 times greater oscillator strength than dye 2 because of its enhanced donor character and interfacial stabilization. This study corroborates the reliability of the $(TiO_2)_9$ as a physically sound minimal model for dye-TiO_2 interfaces. It also establishes a clear design principle: optimizing auxiliary groups for light-harvesting efficiency and interfacial compatibility rather than intrinsic donor strength. This provides a robust foundation for the rational development of sensitizers in dye-sensitized solar cells. These findings suggest that such cluster-based modeling approaches are scalable to larger systems and hold significant relevance for device engineering, enabling more accurate predictions of photovoltaic performance prior to fabrication.

Acknowledgments

This work was funded by the Putian Science and Technology Projects (Grant Nos. 2023GJGZ001, 2023GZ2001PTXY21, and 2025GJJ005).

REFERENCES

1. **Singh, S., Ru, J.** Accessibility, Affordability, and Efficiency of Clean Energy: A Review and Research Agenda. *Environmental Science and Pollution Research International* 29 (13) 2022: pp. 18333 – 18347. https://doi.org/10.1007/s11356-022-18565-9
2. **Patel, D., Patel, S., Patel, P., Shah, M.** Solar Radiation and Solar Energy Estimation Using ANN and Fuzzy Logic Concept: A Comprehensive and Systematic Study *Environmental Science and Pollution Research International* 29 (22) 2022: pp. 32428 – 32442. https://doi.org/10.1007/s11356-022-19185-z
3. **Meng, H., Pang, S., Cui, G.** Photo-Supercapacitors Based on Third-Generation Solar Cells *ChemSusChem* 12 (15) 2019: pp. 3431 – 3447. https://doi.org/10.1002/cssc.201900398
4. **Mahmoud, S.E., Badawy, S.A., Fadda, A.A., Abdel-Latif, E., Elmorsy, M.R.** Triphenylamine-Based Metal-Free Organic Dyes as Co-Sensitizers: Enhancing Dye-Sensitized Solar Cell Performance Through Innovative Molecular Design *Journal of Fluorescence* 35 (11) 2025: pp. 10925 – 10938. https://doi.org/10.1007/s10895-025-04340-9
5. **Thongkasee, P., Thangthong, A., Janthasing, N., Sudyoadsuk, T., Namuangruk, S., Keawin, T., Jungsuttiwong, S., Promarak, V.** Carbazole-Dendrimer-Based Donor-π-Acceptor Type Organic Dyes for Dye-Sensitized Solar Cells: Effect of the Size of the Carbazole Dendritic Donor *ACS Applied Materials & Interfaces* 6 (11) 2014: pp. 8212 – 8222. https://doi.org/10.1021/am500947k
6. **Dos Santos, G.C., Oliveira, E.F., Lavarda, F.C., da Silva-Filho, L. C.** Designing New Quinoline-Based Organic Photosensitizers for Dye-Sensitized Solar Cells (DSSC): A Theoretical Investigation. *Journal of Molecular Modeling* 25 (3) 2019: pp. 75. https://doi.org/10.1007/s00894-019-3958-y
7. **Arooj, Q., Wilson, G.J., Wang, F.** Methodologies in Spectral Tuning of DSSC Chromophores Through Rational Design and Chemical-Structure Engineering *Materials* 12 (24) 2019: pp. 4024. https://doi.org/10.3390/ma12244024
8. **Su, J.Y., Lo, C.Y., Tsai, C.H., Chen, C.H., Chou, S.H., Liu, S.H., Chou, P.T., Wong, K.T.** Indolo[2,3-b]Carbazole Synthesized From a Double-Intramolecular Buchwald-Hartwig Reaction: Its Application for a Dianchor DSSC Organic Dye *Organic Letters* 16 (12) 2014: pp. 3176 – 3179. https://doi.org/10.1021/ol500663b
9. **Cui, H.F., Zhang, K., Zhang, Y. F., Sun, Y.L., Wang, J., Zhang, W.D., Luong, J.H.** Immobilization of Glucose Oxidase Into a Nanoporous TiO_2 Film Layered on Metallophthalocyanine Modified Vertically-Aligned Carbon

Nanotubes for Efficient Direct Electron Transfer *Biosensors & Bioelectronics* 46 2013: pp. 113 – 118. https://doi.org/10.1016/j.bios.2013.02.029

10. **Oprea, C.I., Gîrțu, M.A.** Structure and Electronic Properties of TiO_2 Nanoclusters and Dye-Nanocluster Systems Appropriate to Model Hybrid Photovoltaic or Photocatalytic Applications *Nanomaterials* 9 (3) 2019: pp. 357. https://doi.org/10.3390/nano9030357
11. **Rajkumar, S., Venkatraman, M.R., Arunkumar, A., Jayaprakash, K.** Anthocyanin and Betalain Pigments Assisted Green Synthesis of TiO_2: A Sustainable and Cost-Effective Approach for Dye-Sensitized Solar Cells Photoanodes Panel *Optical Materials* 160 2025: pp. 116710. https://doi.org/10.1016/j.optmat.2025.116710
12. **Huang, J., Li, Z., Yang, L., Hu, R., Shi, G.** A Comprehensive DFT/TDDFT Investigation Into the Influence of Electron Acceptors on the Photophysical Properties of Ullazine-Based D-π-A-π-A Photosensitizers *Scientific Reports* 15 2025: pp. 3101. https://doi.org/10.1038/s41598-025-87189-z
13. **Huang, J., Yang, L., Zeng, S.** Structures and Electronic Properties of Titanium Oxo Clusters With Tartrate Ligand: A Density Functional Theory Study *Materials Science (Medžiagotyra)* 29 (4) 2023: pp. 415 – 420. https://doi.org/10.5755/j02.ms.33426
14. **Huang, J., Yang, L., Chen, Z., Zhou, Y., Zeng, S.** DFT/TDDFT In Silico Design of Ullazine-Derived D-π-A-π-A Dye Photosensitiser *New Journal of Chemistry* 47 2023: pp. 11030 – 11039. https://doi.org/10.1039/d3nj00519d
15. **Kim, M.R., Pham, T.C., Yang, H.S., Park, S.H., Yang, S., Park, M., Lee, S.G., Lee, S.** Photovoltaic Effects of Dye-Sensitized Solar Cells Using Double-Layered TiO_2 Photoelectrodes and Pyrazine-Based Photosensitizers *ACS Omega* 8 (16) 2023: pp. 14699 – 14709. https://doi.org/10.1021/acsomega.3c00707
16. **Huang, J., Yang, L., Zhou, Y., Chen, Y., Liu, Q., Wu, W.** Density Functional Theory/Time-Dependent Density Functional Theory Investigations on the Color-Structure Relationship of Biopigment Molecules. *Journal of Chemical Research* 48 2024: pp. 1–7. https://doi.org/10.1177/17475198231223654
17. **Huang, J., Lv, Y., Wu, J.** Density Functional Theory Calculations on the Solvatochromism of Covalent Organic Framework Py-TT Cluster Compounds *Proceedings of the Royal Society A: Mathematical, Physical and Engineering Sciences* 481 (2311) 2025: pp. 20240768. https://doi.org/10.1098/rspa.2024.0768
18. **El-Shishtawy, R.M., Elroby, S.A., Asiri, A.M., Müllen, K.** Optical Absorption Spectra and Electronic Properties of Symmetric and Asymmetric Squaraine Dyes for Use in DSSC Solar Cells: DFT and TD-DFT Studies *International Journal of Molecular Sciences* 17 (4) 2016: pp. 487. https://doi.org/10.3390/ijms17040487
19. **Sandoval-Salinas, M.E., Brémond, E., Pérez-Jiménez, A.J., Adamo, C., Sancho-García, J.C.** Excitation Energies of Polycyclic Aromatic Hydrocarbons by Double-Hybrid Functionals: Assessing the PBE0-DH and PBE-QIDH Models and Their Range-Separated Versions *The Journal of Chemical Physics* 158 (4) 2023: pp. 044105. https://doi.org/10.1063/5.0134946
20. **Zhang, Y., Li, J., Niu, F., Sun, J., Dou, Y., Liu, Y., Su, Y., Zhou, B., Xu, Q., Yang, Y.** Comparison of a Novel TiO2/Diatomite Composite and Pure TiO_2 for the Purification of Phosvitin Phosphopeptides *Journal of Chromatography. B, Analytical Technologies in the Biomedical and Life Sciences* 960 2014: pp. 52 – 58. https://doi.org/10.1016/j.jchromb.2014.03.038
21. **Liu, Y., Tian, L., Tan, X., Li, X., Chen, X.** Synthesis, Properties, and Applications of Black Titanium Dioxide Nanomaterials *Science Bulletin* 62 (6) 2017: pp. 431 – 441. https://doi.org/10.1016/j.scib.2017.01.034
22. **Alrashdi, S., Casolari, F., Alabed, A., Kyeremeh, K., Deng, H.** Chemoenzymatic Synthesis of Indole-Containing Acyloin Derivatives *Molecules* 28 (1) 2023: pp. 354. https://doi.org/10.3390/molecules28010354
23. **Yin, X., Xue, Z., Wang, L., Cheng, Y., Liu, B.** High-Performance Plastic Dye-Sensitized Solar Cells Based on Low-Cost Commercial P25 TiO_2 and Organic Dye *ACS Applied Materials & Interfaces* 4 (3) 2012: pp. 1709 – 1715. https://doi.org/10.1021/am201842n
24. **Pastore, M., Angelis, F.D.** First-Principles Computational Modeling of Fluorescence Resonance Energy Transfer in Co-Sensitized Dye Solar Cells *The Journal of Physical Chemistry Letters* 3 (16) 2012: pp. 2146 – 2153. https://doi.org/10.1021/jz300839e
25. **Clementi, C., Romani, A., Elisei, F., De Angelis, F., Daus, F., Nunzi, F.** The Dependence of the Spectroscopic Properties of Orcein Dyes on Solvent Proticity: Insights From Theory and Experiments *Physical Chemistry Chemical Physics* 23 (28) 2021: pp. 15329 – 15337. https://doi.org/10.1039/d1cp01535d
26. **Horiuchi, T., Miura, H., Uchida, S.** Highly Efficient Metal-Free Organic Dyes for Dye-Sensitized Solar Cells *Journal of Photochemistry and Photobiology A: Chemistry* 164 2004: pp. 29 – 32. https://doi.org/10.1016/j.jphotochem.2003.12.018
27. **Wen, Y., Wu, W., Li, Y., Zhang, W., Zeng, Z., Wang, L., Zhang, J.** First Principles Study of Thieno[2,3-b]Indole-Based Organic Dyes for Dye-Sensitized Solar Cells: Screen Novel π-Linkers and Explore the Interface Between Photosensitizers and TiO_2 *Journal of Power Sources* 326 2016: pp. 193 – 202. https://doi.org/10.1016/j.jpowsour.2016.07.001
28. **Kim, K.H., Lee, S., Moon, C.K., Kim, S.Y., Park, Y.S., Lee, J.H., Woo Lee, J., Huh, J., You, Y., Kim, J.J.** Phosphorescent Dye-Based Supramolecules for High-Efficiency Organic Light-Emitting Diodes *Nature Communications* 5 2014: pp. 4769. https://doi.org/10.1038/ncomms5769